Computation and Neural Systems

Edited by:

Frank H. Eeckman
Lawrence Livermore National Laboratory

James M. Bower
California Institute of Technology

KLUWER ACADEMIC PUBLISHERS
BOSTON/DORDRECHT/LONDON
1993

78

INTER-AREA SYNCHRONIZATION IN MACAQUE NEOCORTEX DURING A VISUAL PATTERN DISCRIMINATION TASK

Steven L. Bressler

Center for Complex Systems, Florida Atlantic University, Boca Raton FL 33431

Richard Nakamura

Laboratory of Neuropsychology, NIMH, Bethesda MD 20892

ABSTRACT

Synchronization among cortical sites was investigated in a macaque monkey performing a visual pattern discrimination task. Single-site power and between-site coherence were computed from transcortical field potentials. At the time of the behavioral response, power and coherence increased for a select set of cortical sites widely distributed in one hemisphere. The increase was not specific to any narrow frequency band, but occurred over the entire observable range between 0 and 100 Hz.

78.1 INTRODUCTION

Although much is known about the properties of single cortical neurons, relatively little is understood about the cooperation of those neurons in large-scale cortical networks. Yet a leading single-cell neurophysiologist has claimed that in order to understand the relation between cortical function and complex behavior, it is necessary to study the dynamic aspects of network activity [1]. In recent years, inter-area synchronization has received attention as a possible mechanism of cortical organization at the network level.

Most of the work in this field has dealt with correlation of oscillatory activity in the γ frequency range (30-80 Hz) [2]. In the rabbit, olfactory perception during a sniff involves an increase in γ correlation between olfactory bulb and cortex that is location-specific in both structures [3]. In the cat visual system, increased γ correlation in response to coherent visual stimuli has been found between sites within striate cortex [4], between homologous striate sites of left and right hemispheres [5], and between striate sites and several extrastriate areas [6].

In monkeys there is still no consensus on the role, or even the existence, of γ oscillations in the cerebral cortex. On the one hand, it has been reported that γ oscillations transiently synchronize between sites in striate cortex of the macaque [7] and squirrel monkeys [8], between sites in the superior temporal sulcus of the macaque [9], and between sites in pre- and post-central sensorimotor cortex of the macaque, particularly during performance of tasks involving fine finger control [10]. On the other hand, one of these reports [7] found that the greater part of the occipital field potential power was concentrated at the low end of the spectrum, and that, although transitory spectral peaks appeared at multiple and variable frequencies in the γ range, the overall appearance of the average spectrum had the form of "1/f noise". Furthermore, the presence of γ oscillations in macaque visual cortex has been questioned by a report [11] which found a broad-band increase in power, and not an increase in γ-band resonant activity, from areas V1 and MT in response to optimally-oriented light bars. In macaque inferotemporal cortex, this report and others [12], also found very little evidence for visual pattern induced γ oscillations. Another group [13] has reported that oscillations are induced in the macaque temporal pole by familiar visual patterns, but in the Δ, not the γ, frequency range.

This report considers the question of inter-area synchronization of local field potentials (LFPs) from widely separate cortical sites in a macaque monkey performing a visual pattern discrimination task. It is important to study a functionally active monkey because synchronization may only occur transiently in conjunction with specific stages of information processing. The issue of frequency is also important. Those reports finding no evidence for γ oscillations in monkey, without considering functional interrelations between cortical sites, do not address the synchronization question. Correlated activity may be an important aspect of cortical function even if it is aperiodic and broad-band.

78.2 METHODS

Experiments were performed at the Laboratory of Neuropsychology at the National Institute of Mental Health in accordance with institutional guidelines. An adult rhesus macaque monkey was trained to perform a visual pattern discrimination task with a GO/NO-GO response paradigm. The monkey was water deprived to provide motivation for task performance. Its water consumption and behavior were carefully monitored to insure adequate hydration. Computer-generated visual stimuli were presented for 100 msec through a silenced piezoelectric shutter. The head was fixed to a headholder located 57 cm from the display screen, the visual angle being 1°/cm. The stimulus set had four diagonal patterns, each formed by four dots (each 9 mm on a side). Each pattern consisted of two dots at opposite corners of an outer square, 6 cm on a side, and two dots at opposite corners of a concentric inner square, 2 cm on a side. Diagonal lines had the outer and inner square dots slanted in the same direction, diagonal diamonds in opposite directions.

The monkey was trained to readily accept chair restraint and to initiate each trial by holding down a lever with the preferred (left) hand. The intertrial interval was randomly varied between 0.5 and 1.25 seconds. The stimulus was presented approximately 115 msec (varied over 25 msec to avoid line frequency locking) following the start of data collection. On GO trials, a water reward was provided 500 msec after stimulus (diagonal lines) onset if the monkey responded correctly by lifting his hand from the lever before 500 msec. On NO-GO trials, the monkey was required to hold down the lever for 500 msec following presentation of diagonal diamonds. GO and NO-GO trials were randomly presented with equal probability in 1000-trial sessions lasting approximately 35 minutes.

All surgical procedures were preceded by ketamine sedation and pentobarbital anesthesia. Surgical preparation was performed in two stages. First, following craniotomy, recording electrode positions were selected based on the sulcal markings found on the inner cranial surface. Stainless steel screws were inserted in the outer cranial surface at these positions and the calvarium was replaced. Additional screws were placed in the same region for grounding. The cranium was allowed to refuse for one month, after which the second surgical stage was performed to implant the recording electrodes. At each recording site, the screw was removed and an opening was made in the exposed dura. Each electrode consisted of a teflon-coated pair of platinum wires with 2.5 mm tip separation and each tip having a 0.5 mm long exposed surface. The electrode was advanced through the dural opening until the less-advanced tip rested against the pial surface. Electrodes were distributed across the right cortical convexity. They were affixed to the cranium with dental acrylic. The monkey was allowed to recover for at least two weeks before proceeding with data collection.

Results are presented from analysis of two sessions' data collected two weeks apart. The data set consisted of 892 correctly performed GO trials and 901 correctly performed NO-GO trials from 11 intracerebral electrode sites in the right hemisphere (Fig. 78.1): one striate, one prestriate, five parietal, two somatosensory, and two motor. Simultaneous transcortical LFPs were recorded by bipolar differential amplification using Grass Model 7P511J amplifiers with passband between 1 and 100 Hz (3 dB points). Digitization was at 200 samples/sec for each channel. Gain settings were individually adjusted for each channel to maximize signal amplitude without clipping. Gain correction was applied to each record to recover the original signal strength in microvolts, and a digital 60 Hz notch filter was applied to remove the effect of line-frequency contamination.

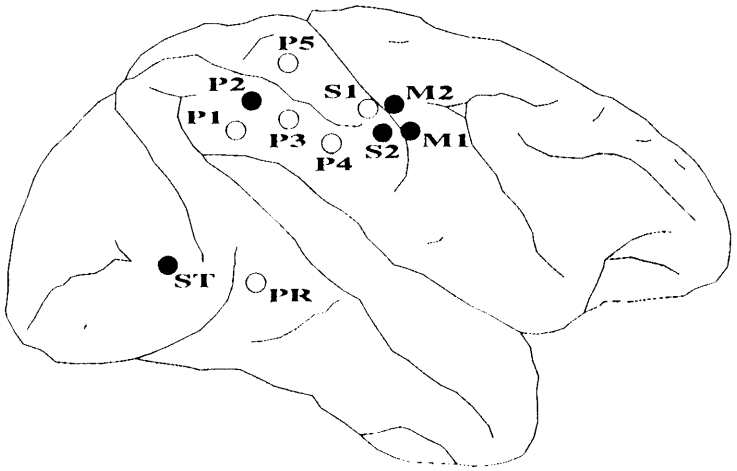

Figure 78.1 Eleven electrode sites were monitored in right cortical convexity of the rhesus macaque monkey. (ST: striate; PR: prestriate; P1 - P5: parietal; S1 - S2: somatosensory; M1 - M2: motor.) Closed circles: 5 sites (group A) in session 1 were synchronized during the response. Open circles: Non-synchronized sites (group B).

78.3 RESULTS

Average Potentials

The peak amplitudes of the post-stimulus average LFPs were in the range of 200-2000 μV. The components generally were of three types: an early negative peak (N1) at or prior to 200 msec, a mid-latency positive peak (P2) prior to 300 msec, and a late broad component after 300 msec. The GO and NO-GO average waveforms were highly similar for at least the first 150 msec post-stimulus at all sites. In session 1, four sites (parietal sites 1,3,4,5) showed only small between-condition differences in waveshape, and no long-lasting between-condition divergence. At the other sites, a distinct divergence began from 165 to 280 msec, a period prior to, and overlapping, the response onset in the GO condition (265 +/- 16 msec). Five of these sites (striate, parietal 2, somatosensory 2, and motor 1 and 2), were distinguished by the GO waveform showing a distinct peak at 345 msec, followed by a slow return toward baseline, that was absent in the NO-GO condition. This group of five sites (group A) thus had important similarities during the response, not shared with the other six (group B). In session 2, the distinction between groups A and B persisted, except that group A expanded to include parietal site 3, which had previously been in group B.

Power

To compare the frequency content of the GO and NO-GO event-related LFPs, the Discrete Fourier Transform (DFT) was computed for the time window consisting of the first 500 msec post-stimulus of each trial. The GO and NO-GO power spectra were averaged for each site and the natural logarithm was applied. These spectra decreased with increasing frequency in a characteristic "1/f" manner. Overall, the power of group A sites was significantly greater than group B by the Student's t-test (session 1: $t=2.33$, $p < 0.05$; session 2: $t=12.04$, $p < 0.01$; d.f.$=9$). In addition, power in the GO condition was greater than the NO-GO condition for all group A sites, the difference being significant (session 1: $t=4.60$, $p < 0.01$; session 2: $t=5.37$, $p < 0.01$; d.f.$=9$) as compared to group B.

For more precise localization of the time when the spectra of the two conditions differed, average DFTs were again computed, but now for 113 windows, each 80 msec long, centered from 60 msec pre-stimulus to 500 msec post-stimulus. The windows were highly overlapped, each differing from the previous by only one point. The greater temporal resolution resulted in relatively poor frequency resolution, the time window of 80 msec yielding frequency bins at 12.5 Hz intervals. Log power was displayed separately for each frequency bin as a time-series where each point corresponded to the center of one of the 113 windows. (The 0 Hz bin was excluded because of d.c. offset artifact, and the 100 Hz bin was excluded because of poor resolution at the Nyquist frequency.)

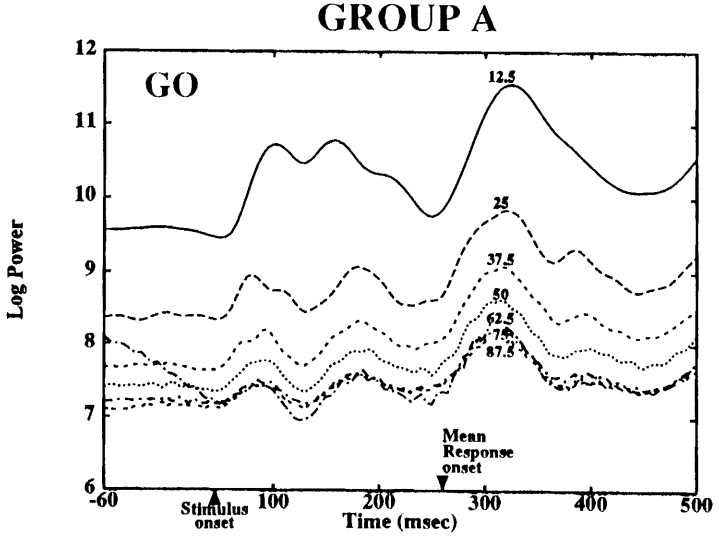

Figure 78.2 Average group A log power for each frequency bin as a function of time. The peak in power (310-325 msec) during the behavioral response was specific to group A sites. Power time-series are labeled in Hz by frequency bin.

The power time-series results were in general agreement with those of the amplitude averages, but showed that the late response-related components seen at group A sites consisted of power across the whole observable spectrum (Fig. 78.2). The major difference between conditions, like the amplitude averages, occurred in group A and consisted of an increase in power with the behavioral response for all frequencies in the GO condition. This change was not observed for group B.

Coherence

The average LFP waveforms indicated that at the time of the response in the GO condition an event took place that was similar at group A sites. Power spectral analysis suggested that this similarity extended across the observable frequency spectrum (0 - 100 Hz). However, single-site amplitude or power measures do not measure similarity directly. For this, the coherence spectrum [14], a measure of waveshape similarity, was employed. Coherence spectra of all 55 pairwise combinations of the 11 sites were computed for each of the same 113 80-msec-long windows that had been used to compute power spectra.

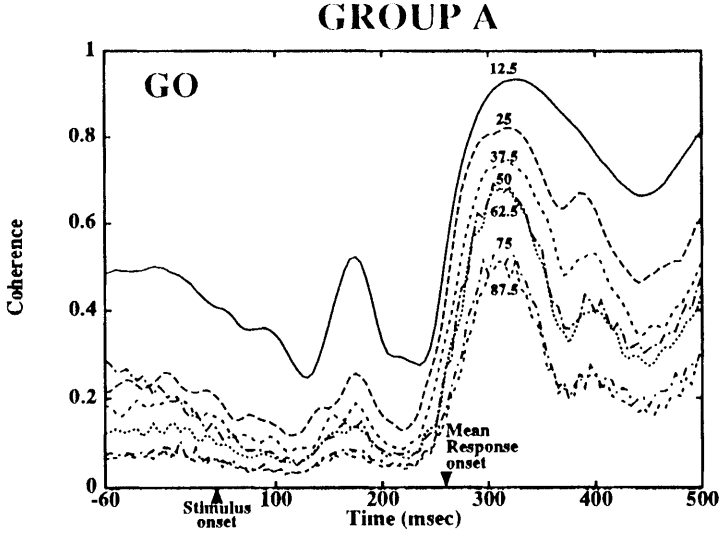

Figure 78.3 The average group A coherence time-series displayed for each frequency bin. The large broad-band increase in coherence with the behavioral response (GO condition) was specific to group A sites. Coherence time-series are labeled in Hz by frequency bin.

From the coherence spectra, coherence time-series were constructed for each available frequency bin. These coherence time-series were averaged for all within-group site pairs, yielding group A and group B average coherence time-series.

Since, by definition, coherence values lie within the range of 0 to 1, the Fisher z-transform, which converts a bounded distribution to an unbounded one, was used before averaging coherence.

The post-stimulus temporal course of coherence conformed to what was expected from the power time-series results. Group B mean coherence was uniformly low (below 0.2) at all frequencies in both conditions. For group A, mean coherence followed the same basic temporal pattern for all frequencies. In both conditions, group A coherence declined following the stimulus. In the GO condition, it then greatly increased beginning shortly before response onset and peaked near 325 msec (Fig. 78.3). NO-GO coherence remained low at this time. For both sessions, the coherence in the GO condition at 325 msec was significantly higher than the pre-stimulus level when compared to the group B pre-/post-stimulus difference (session 1: $t=28.90$, $p < 0.01$; session 2: $t=8.95$, $p < 0.01$; $d.f.=23$). The expansion of group A in session 2 to include parietal site 3 was confirmed by its high coherence with the other group A sites.

78.4 DISCUSSION

The most important finding of this study is that multiple, distributed sites in the monkey neocortex can become functionally linked in large-scale networks during visual task performance. The increase in coherence of group A sites at the time of the response suggests that inter-area synchronization is involved in task performance and that an extended cortical network serves to process task information.

The increase in coherence was spatially selective. Out of the eleven sites available, only five sites (group A) in session 1 became linked at the time of response onset. Spatial specificity was particularly evident in parietal cortex, where only one site out of five in session 1 was linked in the global network. Presumably the same degree of specificity was present in other cortical regions (e.g. striate cortex), although it could not be observed due to the limited number of electrode recording sites. Assuming adequate spatial sampling, the spatial pattern of coherence may be a sensitive indicator, at each successive processing stage, of those sites that are functionally linked in a cortical network.

The coherence peak was spectrally broad rather than being confined to narrow spectral peaks. When group A coherence increased with response onset, it did so over the entire range of observable frequencies, indicating that narrow-band oscillations are not a prerequisite for inter-area synchronization in a cortical network. That synchronization appears even at the low end of the spectrum implies that it is accessible in human scalp-recorded brain potentials, and lends credence to studies which have shown discrete spatial covariance patterns from the human brain related to specific stages of information processing [15].

Acknowledgement

Supported by NIMH Grant 43370 to EEG Systems Laboratory, San Francisco CA. We thank Don Krieger for assistance in data transfer.

REFERENCES

[1] Mountcastle, V.B. In *The Mindful Brain*, G. Edelman (Ed.) MIT Press, Cambridge (1979) 7.

[2] Bressler, S.L. & Freeman, S.L. *Electroencephalogr. Clin. Neurophysiol.* **50** (1980) 19; Bressler, S.L. *Trends Neurosci.* **13** (1990) 161.

[3] Bressler, S.L.. *Electroencephalogr. Clin. Neurophysiol.* **57** (1984) 270; Bressler, S.L. *Brain Res.* 409 (1987) 285; Bressler, S.L. *Brain Res.* **409** (1987) 294; Bressler, S.L. *Behav. Neurosci.* **102** (1988) 740.

[4] Gray, C.M., Konig, P., Engel, A.K. & Singer, W. *Nature* **338** (1989) 334; Gray, C.M., Engel, A.K. Konig, P. & Singer, W. *Visual Neurosci.* **8** (1992) 337; Engel, A.K., Konig, P. & Singer, W. *Proc. Natl. Acad. Sci. USA* **88** (1991) 9136.

[5] Engel, A.K., Konig, P., Kreiter, A.K. & Singer, W. *Science* **252** (1991) 1177.

[6] Eckhorn, R., Bauer, R., Jordan, W., Brosch, M., Kruse, W., Munk, M. & Reitboeck, H.J. *Biol. Cybern.* 60 (1988) 121; Engel, A.K., Kreiter, A.K., Konig, P. & Singer, W. *Proc. Natl. Acad. Sci. USA* **88** (1991) 6048.

[7] Freeman, W.J. & van Dijk, B.W. *Brain Res.* **422** (1987) 267.

[8] Livingstone, M.S. *Soc. Neurosci. Abstr.* **17** (1991) 176.

[9] Kreiter, A.K. & Singer, W. *Europ. J. Neurosci.* **4** (1992) 369.

[10] Murthy, V.N. & Fetz, E.E. *Proc. Natl. Acad. Sci. USA* **89** (1992) 5670.

[11] Young, M.P., Tanaka, K. & Yamane, S. *J. Neurophysiol.* **67** (1992) 1464.

[12] Gawne, T.J., Eskandar, E.N., Richmond, B.J. & Optican, L.M. *Soc. Neurosci. Abstr.* **17** (1991) 443; Tovee, M.J. and Rolls, E.T. *Neuroreport* **3** (1992) 369.

[13] Nakamura, K., Mikami, A. & Kubota, K. *Neurosci. Res.* **12** (1991) 293.

[14] Glaser, E.M. & Ruchkin, D.S. *Principles of Neurobiological Signal Analysis*, Academic Press, New York (1976) 174.

[15] Gevins, A.S. & Bressler, S.L. In *Functional Brain Imaging*, G. Pfurtscheller & F.H. Lopes da Silva (Eds.) Hans Huber Publishers, Bern (1988) 99.